A Review of Recent Advancements in Flux Reversal Permanent Magnet Machine (FRPMM)

Manne Bharathi, M. Kiran Kumar, O. Chandra Sekhar, M. Ramamoorty

Abstract: ***The flux reversal permanent magnet machine (FRPMM) is a novel brushless double-salient permanent-magnet machine with a winding less rotor, in which phase flux polarities are reversed in the stator concentrated coils for each electrical cycle of rotor displacement. In this concept, the qualitative comparisons are made between the FRM with different varieties of brushless machines, especially a switched reluctance machine based on Flux-MMF diagram technique. This description gives the all-inclusive review of improvements of several electrical machines for adoption to renewable energy harvesting, disclose all equivalent limitations along with research favorable circumstances. Various design strategies such as the magnet arrangement, winding techniques are adopted to increase the performance of FRPM and key results have been discussed and analyzed.***

Index Terms:FRPMM, FMDT (Flux-MMF Diagram), Design procedure, Cogging Torque, Permanent magnet Arrangements.

I. INTRODUCTION

Flux Reversal Machine (FRM) was invented in the year 1997 by R.P. Deodhar and et al with the concept of including the benefits of switched-reluctance and permanent-magnet (PM) machines having high torque density [1]. The FRPMM is not the first doubly-salient PM machine which contains static permanent magnets integrated with a basic variable unexcited reluctance rotor, it seems that it is the first to contain bipolar MMF along with flux variation with rotor displacement. It seems that FRPMM contains less inductance by nature, hence electrical time constant is less. The characteristics, integrated with the easy or basic built, result in high fault tolerance, simple maintenance, quick transient response and low rotor inertia [2]. Thus, FRPM machines became attractive for low speed and high-speed traction applications especially for electrical vehicle propulsion [4], automotive drive and wind power generation systems [6] and low-speed servo systems [7]. There are several researchers worked on the design and analysis of FRPMMs. A subjective comparison was made among the FRM and few different types of brushless machines, along with double salient PM machine (DSPMM) and SRM [8] with respect to operating principle, inductance, torque capabilities, etc. Comparativeperformance of FRPM machine and DSPM machine has been evaluated in [9]. To improve the torque density of FRPMM, several novel methodologies were being adopted such as separate PM excitation stators of FRPMM [10], novel dividing up flux reversal machine (PS-FRPM) with Consequent-pole PM stator (CPM) [11], etc. By using full pitch winding concept of FRPMM, which increases the output power double that of conventional FRPMM with Concentrated stator pole winding [12]. However, due to double salient structure few FRPMMs withstand from cogging torque, which generates vibrations, noises while diminishing the machine performances. Therefore, so as to reduce the cogging torque some more design changes are considered such as skewing [13], dummy slots [14], bifurcated asymmetrical rotor teeth [15], rotor teeth pairing [16] and chamfering of permanent magnet [17], etc. The conventional FRPMM coupled to fictitious 'Electrical Gear' have been evaluated based on flux pattern of the machine [18]. It was found that the FRPMM can exhibit similar torque production mechanism as in Vernier machine and magnetic geared machine [19]-[20]. Hence, it is most suitable for direct-drive-rooftop wind power generation. In various technical articles, the particular model of FRMs is mostly dependent on the conventional model by using FEA(finite element analysis)since the analytical methods cannot be applied directly. In this review paper of FRPMM attempt has been made to make a comprehensive presentation on construction, working principle, comparative evaluation with other type of brushless machines, design procedure, performance analysis and improvement methods of FRPMM and also reviews the recent advancements in FRPMM algorithms especially in renewable energy harvesting and automotive industry.

In this paper the concept is dividedas follows. The construction and basic working principle of FRPMM is discussed in section 2. The comparison of FRPMM with various types of machines based on Flux-MMF diagram is made in section 3. Whereas, in section 4, design procedure ofFRPM machine with stator and rotor geometric parameters is illustrated. Section 5, different strategic design to improve performance characteristics of FRPMM like stator winding and magnet arrangement techniques are analyzed.In section 6, applications of FRPM machine is are discussed. Finally, conclusions are drawn in section 7.

Revised Manuscript Received on March 20, 2019.

Manne Bharathi, EEE, KLEF, Guntur, India.
M. Kiran Kumar, EEE, KLEF, Guntur, India.
O. Chandra Sekhar, EEE, NIT, Srinagar, India.
M. Ramamoorty, EEE, Former Chancellor of KLEF, Guntur, India.

II. PRINCIPLE OF OPERATION

The basic working principle of FRPMM is analogous to BLDC motor. The major variation is that FRM is rugged and effortless to manufacture, because of its PMs placed on the stator pole shoes or in the stator pole surfaces. The FRM working principle is based on flux linkage which varies, producing an EMF that interacts with armature current.

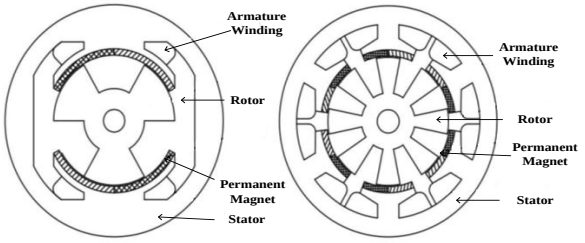

(a) **(b)**

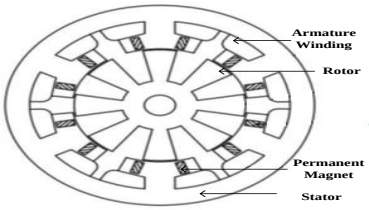

(c)

Fig. 1.Cross-sectional view of an FRPMM (a) 2/3-pole. (b) 6/8-pole,(c) 6/8- pole, PMs in stator pole shoes.

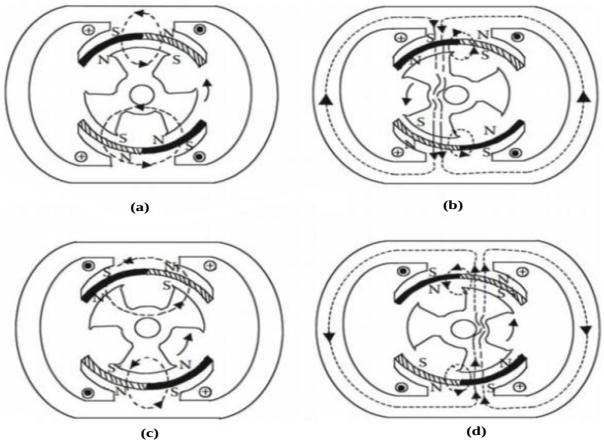

Fig. 2. Operating rule of FRPM machine. (a) Position of zero flux linkages, (b) position of a maximum-positiveflux linkages, (c) position of zero flux linkage, and (d) position of negative-maximum flux linkages.

"Fig. 1," has the cross sections of FRPM machines of a 1φ with a three-pole variable reluctance rotor and a two-pole stator, six-pole stator, eight-pole rotor and with PMs in stator pole shoes both of salient nature. On every stator pole face the Two arc magnets are placed one beside the other of opposite polarity. Every pole of a stator coil is concentrically wound and they form a single-phase winding when they are connected in series. The operating principle of FRPM machines are not restricted to single-phase machines but also identically valid for multi-phase machines like three-phase, five-phase etc.

"Fig. 2" describes the difference of flux and current, where fig.3explains the changes in MMF and phase-flux with rotor movement for two electrical cycles. Observe that all the phase flux linkages are plotted based on "per-turn" [1]. The count of energy cycles could be increased by increasing the rotor pole number. The phase-flux and MMF variations are bipolar, current is alternating (Square wave). For each electrical cycle of rotor movement, the sign isreversed by phase-flux as it can be viewed in figs 2 and 3.

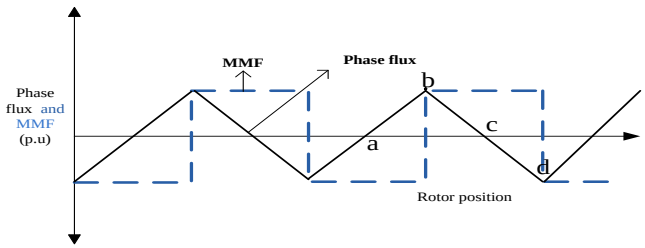

Fig. 3. The change scale of phase-flux and MMF with rotor position of an FRPMM.

Considering flux-reversal machine is unexcited and the rotor is rotated in anti-clockwise direction. In fig. 2(a) the rotor is in the equilibrium position, there is no flux linked with the stator coils. The flux linkage of the coils in this position is zero (point(a) in fig. 3). And in fig. 2(b), displaced a rotor from 30deg anti-clockwise direction, so that the rotor poles are overlaps with the magnets present in the stator poles. Then now the flux links with the stator coils, the flux is maximumpositive at this position (point(b) in fig. 3). In fig. 2(c), the rotor is at the position of equilibrium, rotated by 60deg from an original position. Again, there are no flux links with the stator coils(point(c) fig. 3). A further movement of the rotor of 30deg in anti-clockwise direction leads to the positionin fig. 2(d). Then the flux links with the stator coils again, the flux is again negative-maximum(point(d) fig. 3). Thus, in one rotor revolution, the stator coils exhibit three cycles of flux linkage variations for each an electrical cycle comprising of change from zero to maximum-positive, from maximum-positiveto zero, from zero to maximum-negative, and from maximum-negative to zero. The linear variation of a bipolar phase-flux (ideally a triangular wave) and MMF (square wave) results in a trapezoidal EMF. Appling Faraday's law, which is given in fig.3. The maximumEMF at (a), maximum-negative (c), and zero at (b) and (d).

III. COMPARISON WITH DIFFERENT DOUBLE SALIENT MACHINES

Performance comparison of different machines can be made on the basis of operational characteristics, torque-ripple, magnetic and electric loadings. Comparison is made between Switched reluctance machine (SRM), BLDC machine, DSPM machine, and FRPM machine, by using Flux-MMF diagram technique (FMDT). The FMDT evolution depends on principle of virtual work, based on an ideal change of MMF and phase-flux per phase over an electrical cycle. This is utilized to evaluate the converted energy and the instantaneous and average torque developed.

"Fig.4," gives the cyclic change of MMF and phase-flux with rotor displacement for four types of double salient machines were utilized to compare. Fig. 5, depicts how the FMDT for every machine can be plotted with the help of the change of MMF and phase-fluxin fig. 4.The area covered by the flux-MMF loop represents the energy converted during an electrical cycle and also represents the electromagnetic torque generated during the coincide with movement. Observe the total value of net MMF and phase-flux changes during an electrical cycle is supposed to be same for each machine.

Table 1. Differentiation among the FRPMM and several brushless machines.

Design Issue	DSPM	SRM	BLDC	FRM
PMs	PMs in stator or rotor yoke	No	PMs in the rotor	PMs in the stator pole surface
Flux variation	Uni-polar	Uni-polar	Bi-polar	Bi-polar
Field winding	No	No	No	No
Energy	First and	First	All four	All four
Power density	High	Low	Very High	Veryhigh
Cogging torque	Medium	No	High	High
Rotor inertia	Low	Low	Medium or high	Low
MMF variation	Bipolar	Uni-polar	Bipolar	Bipolar

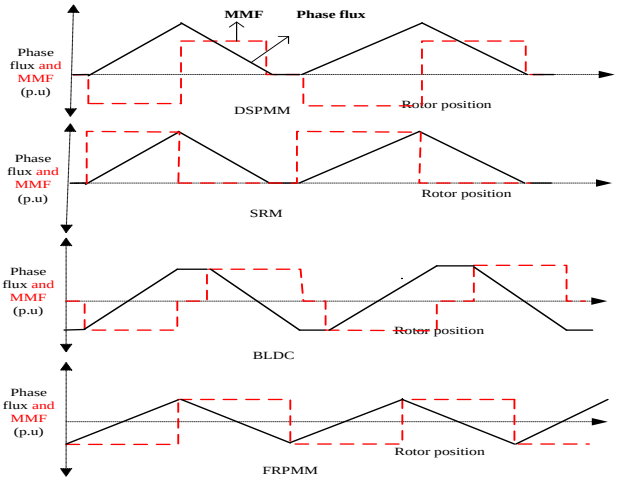

Fig. 4. The phase-flux and MMF difference withposition of the rotor for various types of brush less machines.

A. Some important concepts to be identified on the comparative calculation of each of the four machines

- The DSPM has bipolar MMF variation and unipolar phase-flux variation, where the SRM contains unipolar MMF and phase-flux variation. The BLDC, FRPMM both have bipolar MMF and phase-flux variations.
- In the instance of DSPMM, the energy-conversion loop is restricted to initial two quadrants, whereas for the SRM, the loop of energyconversion restricted to first quadrant only. In BLDC and FRPMM, loop of energy conversion covers all four quadrants and energy conversion is possible in all four quadrants.
- Unlike BLDC Motor where Pole is fixed in stator making the structure easy to fabricate.

Because of the above reasons FRPPM is gaining importance in Industry and Transport applications.

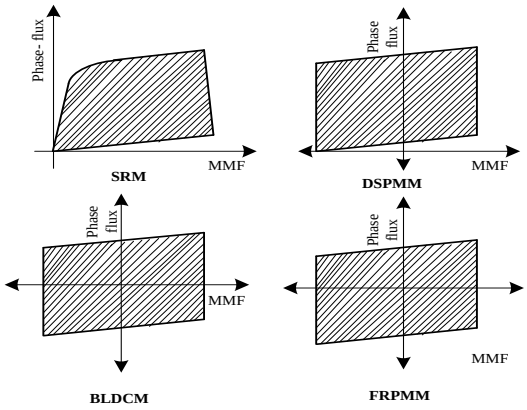

Fig. 5. Comparison between SRM, DSPM, BLDC and the FRPMM, by using FMDT.

IV DESIGN PROCEDURE FOR FLUX REVERSAL MACHINE

A. Basic Configuration

i. Relation between number of Stator and Rotor poles

For evaluating the count of rotor and stator poles, consider the schematic diagram of FRPMM as shown in fig.1(a).As air gap is very less compare to rotor diameter air gap length 'g' can be neglected and then circumference of the inside of stator and rotor will be equal, giving the relation of stator and rotor poles N_r [21].

$\pi D_r = 2\ N_r T_p$ (1)

The perimeter of the stator poles will be the sum of the poles and the space between the poles. The space between the adjacent poles will be $2N_sT_p/3$ (equivalent to 120 Elec. degrees) and the sum of the poles will be $2N_snpT_p$. The perimeter of rotor poles with diameter $D_r + 2g$ is given

$\pi(D_r + g) = 2N_snpT_p + 2N_sT_p/3$(2)

Neglect the airgap 'g' and then equate the equations (1) and (2) to get

$2\ N_rT_p = 2N_snpT_p + 2N_sT_p/3$ (3)

The relation between the number of rotor and stator poles is expressed as

$N_r = N_s\ (np + \frac{1}{3})$ (4)

Where, N_r = stator poles number

N_s= rotor poles number

T_p= pole pitch of rotor.

Published By:
Blue Eyes Intelligence Engineering
& Sciences Publication

np= count of magnet pairs per pole.
D_r= Rotor diameter.
g=Airgap length

For theconventional configuration as in fig.1(a) the count of poles of a stator is 2 and the count of magnet pairs per pole 1 and found that 3 rotor poles are required from equation (4). This evaluation is applicable to all FRPMM configurations.

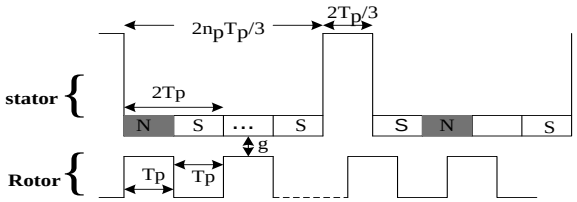

Fig.6. Linear cross-section of FRPMM.

B. Structural design of Stator and Rotor

Sizing equation of FRPMM procedure is useful for determining the stator and rotor geometrical parameters. The geometrical view of stator and rotor given in fig.7. Fig.8 depicts the design process of FRPMM can be analyzed by flow-chart [18].Variables used in the fig.7 are defined as follows:

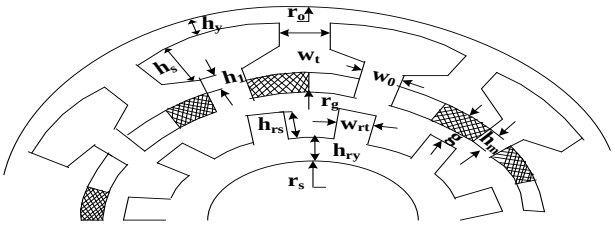

Fig. 7. Geometrical view of stator and rotor.

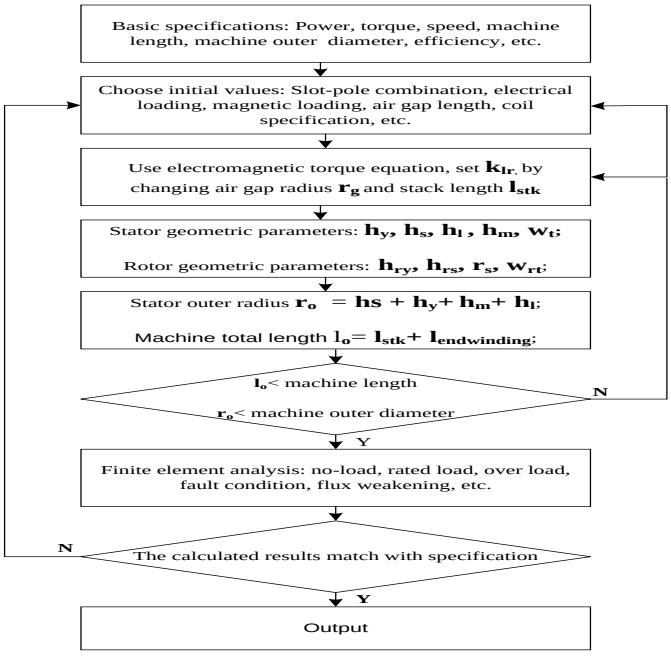

Fig.8. Design flow-chart of FRPMM.

Where, r_o= Stator outer radius;
r_g= Air gap radius;
g = Air gap length;
l_{stk} = length of the Stack of a machine;
k_{lr} = The ratio of $r_g$to l_{stk} ;
h_y= Thickness of stator yoke;
h_m= PM radial thickness;
h_s = Stator slot depth;
w_t = Tooth width of stator;
w_o = Slot opening width;
h_{ry} = Rotor yoke thickness;
h_{rs} = Rotor slot depth;
w_{rt}= Tooth width of rotor;
A_e = Electrical loading;
B_m =Equivalentmagnetic loading.

i. Stator geometric parameters design

The stator winding flux per pole with zero-load condition can be written as

$$\phi_m = 2\,\lambda_w B_m\, l_{stk}/3 \qquad (5)$$

Where λ_w is winding pitch, assume stator winding is full-pitched one, the winding pitch can be expressed as

$$\lambda_w = \pi r_g/p \qquad (6)$$

Then stator winding flux per pole equation (5) can be rewritten as

$$\phi_m = 2r_g B_m\, l_{stk}/p \qquad (7)$$

When stator yoke flux density is supposed to be B_y, the stator yoke thickness will be obtained as

$$h_y = \frac{\phi_m}{2B_y l_{stk} K_{stk}} = \frac{r_g B_m}{P B_y K_{stk}} \quad (8)$$

Similarly, If the stator teeth flux density is supposed to be B_t, the stator tooth width will be derived as
Where, SPP = Slot per pole per phase,

$$w_t = \frac{\phi_m}{3SPP\, B_t\, l_{stk} K_{stk}} = \frac{4r_g B_m}{Z_s B_t K_{stk}} \quad (9)$$

However, a thick permanent magnet implies a higher cost. Magnets used in the machine is Nd FeB 52 MGOe. In order to decrease the chance of PM demagnetization and to maximize the torque density, The PM thickness is generally selected as

$$h_m = 4g \sim 6g \qquad (10)$$

If ratio of slot opening is approximately 0.25 [3], torque density goes to maximum value.
The slot opening width of stator

$$w_o = \pi(r_g + h_m)/2Z_s \qquad (11)$$

The complete slot area of FRPMM is given depending upon the electrical loading A_e and the current density J_e. If the current density is high, it decreases the machine time constant and size, reduces the efficiency. A Corresponding low time Constant increases the commutation process. The base current density is chosen approximately as $J_e = 6\ A/mm^2$.
The overall area of the slot FRPMM is expressed as

$$A_{slot} = 2\pi(r_g + h_m)A_e/J_e S_{fg} \quad (12)$$

In which, S_{fg} is the slot fill factor. Low fill factor can be chosen as S_{fg} = 0.38.

Published By:
Blue Eyes Intelligence Engineering
& Sciences Publication

Moreover, the total slot area can be figured out using the geometric parameters of the stator.

$A_{slot} = \pi(r_g + h_m + h_s + h_1)^2 - \pi(r_g + h_m + h_1)^2 - Z_s h_s w_t$ (13)

Equating (12) and (13), the depth of the slot can be obtained. Then, the outer radius of the stator r_o can be given as

$$r_o = (r_g + h_m + h_s + h_1 + h_y) \quad (14)$$

ii.Rotor geometric parameters design

When the density of flux in a rotor yoke let as B_{ry}, the height of the rotor yoke can be derived as

$$h_{ry} = \frac{r_g B_m}{B_{ry} K_{stk} Z_r} \quad (15)$$

In case the density of flux in rotor teeth is supposed as B_{rt}, the tooth width of the rotor is given as

$$w_{rt} = \frac{4 r_g B_m}{Z_r B_{rt} K_{stk}} \quad (16)$$

Then, the rotor slot depth h_{rs} can be calculated as

$$h_{rs} = r_s + h_{ry} \quad (17)$$

In order to reduce windage loss, a lightweight non-magnetic material is used to fill the inter-pole areas. The rotor contains 8 inter-poles and 8 poles. The machinecore is considered by the shaft by r_s and h_{ry}. The angles suspended by the inter-pole is β and pole is α. The inter-polar area is rounded off near the back iron to diminish the fringing [19].

V. DESIGN TECHNIQUES

The winding of a stator and a magnet arrangement procedure is adopted to increase the machine performance [21]. The rotorand stator salient pole having a type of concave and including a flux obstacle on its edge. The obstacle and concave shapes have a vital role to minimize the leakage flux [22]. The leakage flux decreases the performance of FRPMM in relations of power and torque densities. To examine the characteristics of an FRPMM machine like cogging torque and iron loss [23]. The effect of Cogging torque depends on the stator-rotor pole geometry of the machine. The PMs height (or thickness) of the stator poles and stator geometry are used to minimize the cogging torque. Regarding to geometry of a rotor, the following cases are considered i) V-shaped punches on the rotor pole, ii) Rotor pole arc variation also minimizes the cogging torque. It corresponds to decrease the total cogging torque of a machine can be an impact of A) PM height variation of stator, B) a V-shaped punches on rotor pole, C) rotor pole arc variation.

A. Stator PM height Variation

The Permanent magnet Height increases may result in a greater cost. Usually, PM height is lower results in lesser cost and corresponds to low cogging torque but de-magnetization problems can be occurred when the permanent magnet height is very low. Taking these into consideration, the Parameters of an air gap, rotor and overall dimensions of the machine maintained at the proper way to get an overall performance of the machine will be good. When the permanent magnet height will change, corresponding changes will be in stator pole shoe height. The Permanent magnet height effect on cogging torque can be observed when the PM height values between 2mm and 5mm. The design for various PM heights, corresponding the subsequent changes in the stator pole surface thickness can be seen in fig. 9. The cogging torque for various PM heights can be indicated in fig.10. The cogging torque will be decreased if the PM heights decreased from 5mm to 2mm and the corresponding reduction of torque ripple. There is an increase the flux linkage of the machine if there is an increase in height of PM. This increment of flux linkage which corresponds to the reduction in thecogging torque. Comparatively to the traditional model, 61% of cogging torque can be reduced when the permanent magnet height will be 2 mm [21].

Compared to the various PM heights, 2mm height magnet will decrease both cogging and ripple torque in the machine. Lower the PM heights will lead to maximum power and efficiency.The PM height will increase, losses in the machine increases and corresponding reduction in the machine efficiency. Therefore, the maximum PM height of the FRPMM is 2mm.

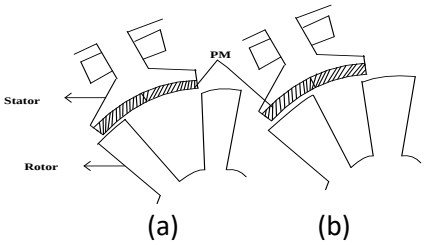

Fig. 9. Height variations of Permanent magnet: a) 2 mm, b) 5 mm.

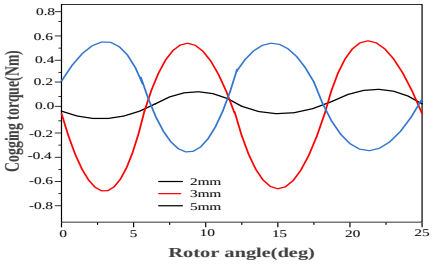

Fig.10. Cogging-torque for various PM heights, 2mm, 3mm and 5 mm.

Table 2. Cogging torque for different PM heights.

S.NO	height of Magnet	Cogging-torque(Nm)
1	2mm	0.05
2	3mm	0.45
3	5mm	0.53

B. V-Shaped punches on rotor poles

The measurements of v-shaped punches on the poles of rotor changes but PMs and stator structures are not varied. The punching hole depth h_d, the gap amongthe rotor pole tip $h_l$and punching hole, and the opening width of holeh_w are the very prominent limitations of the v-shaped holes on the rotor poles.The $h_d$ranges from 0.34 to 3.73mm, with a step variation of 0.5mm. The h_l ranges from 0.38 to 4mm, with a step variation of 0.53mm and also the h_w rangesfrom 0.38 to 4mm, with a step variation of 0.53mm [22].

Cogging torque is primarily decreased if the width and depth of the hole-punchis decreased and the gap increases from the

hole to the tip of rotor pole. The structure view of double punches on rotor poles dimensions are indicating fig. 11. Cogging for various rotor punchingmagnitudes is given in fig. 12.

If the hole depth decreases, the reluctance path increases and the magnetic flux decreases. Therefore, cogging torque and leakage flux is decreased. If hole depth of a pole is very deep, i.e. h_d = 3.73, the paths of flux are confined to the thinsegment in thepole of rotor. Thus, the decrement in a torque and correspondingrising in theripple of torque.

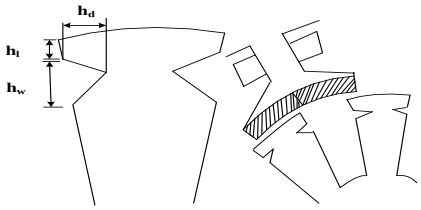

Fig. 11. Structural view of V-shaped punches on poles of rotor.

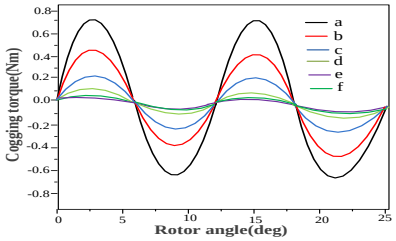

Fig. 12. Cogging-torque of various punch-hole dimensions. a)h_d = 3.72 mm, h_w= 4 mm,h_l= 0.38 mm b)h_d = 3.24 mm, h_w= 3.52 mm, h_l = 0.9 mm c)h_d= 2.72 mm, h_w= 3 mm, h_l = 1.41 mm d) h_d = 2.25 mm, h_w= 2.47 mm, h_l = 1.91 mm e)h_d = 0.85 mm, h_w= 0.92 mm, h_l= 3.58 mm e)h_d = 0.34 mm, h_w= 0.39 mm, h_l = 4 mm.

If the depth of hole in a pole is very deep, i.e. h_d=0.3mm, the flux flows through the wider portion in the rotor pole. Therefore, torque ripple decreases in the machine such as in the non-v-shaped punched rotor pole similar to a conventional flux reversal machine. However, low torque ripple and high average torque will be obtained at a h_d of 0.82mm. Therefore, the optimum punchinghole dimensions to reduction in the cogging and torque ripple are h_d = 0.82mm, h_l =3.48mm, and h_w = 0.9mm. In comparison to the traditional method, the cogging-torque can be decreased 84% in the v-shaped punch model. When the hole depth is decreased, the losses are very less and corresponding improvement in the machine's efficiency.

C. Rotor pole span angle (β_r) variation

The rotor pole span angle β_r contains excessive effect on the cogging-torque [24]. The impact of changing β_r is studied, when maintain the magnet arc to be constant. The β_r changes in the range of 15.5^o to 25.5^o. The pole arc with 15.5^o and 25.5^o, in each instance in fig.13.

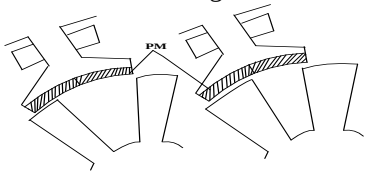

(a) (b)

Fig. 13. Arc of a rotor pole FRPMM.**a)**arc of a pole 15^0, **b)** arc ofpole25.5^0

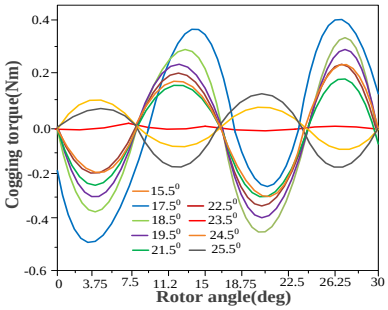

Fig. 14. Cogging torque of various pole arcs, $15^0<\beta_r<25.5^0$.

Table3. Cogging-torque for various arcs of a rotor pole**.**

S.NO	The pole of a rotor span angle (degree)	Cogging-torque (Nm)
1	15.5	0.15
2	17.5	0.3
3	18.5	0.28
4	19.5	0.22
5	21.5	0.29
6	22.5	0.13
7	23.5	0.013
8	24.5	0.06
9	25.5	0.2

Minimum ripple and cogging torque caused at the pole of a rotor span angles from 23.5^0 to 25.5^0. Which in turn shows that if rotor pole arcs are higher, it is helpful in decreasing the reluctance torque in the machine and also reduces cogging torque. Maximum-efficiency can be achieved at the arc ofa rotor pole is 23.5^o. Thus, the optimumarray of pole of a rotor span angle for the machine is 23.5^o to 25.5^o.

D. Combined Optimized Parameters Model

The models like Stator PM height variation, v-shaped punches on a pole of a rotor, and rotor pole arc difference techniques has a better depletion in cogging-torque, particularly in 23.5^o rotor pole span angle method, where cogging-torque can be nearly completely eliminated. Where the PM height and rotor pole arc are significant to attain an average torque by decreasing in cogging torque. The Permanent magnet height technique has the minimum chance of decreasing the cogging comparatively to the other techniques. Both rotor punch and the rotor pole arc techniques have alike ripple torque, whereas the cogging-torques of a v-shaped punched method is somewhat more than the β_r method.

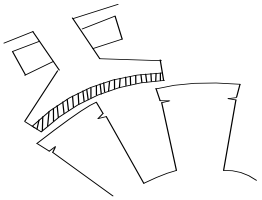

Fig. 15. Combined optimized model.

Combinedoptimized parameter model is shown in fig. 15. This FRPMM model has a βr of 23.5°, a height of PM is 2 mm and a v-shaped rotor punches width h_w = 0.9 mm, h_l= 3.48 mm, and h_d= 0.82 mm. Cogging-torque for an optimized model is shown in figure 16. This Combined model has more torque-ripple than the other optimized methods.

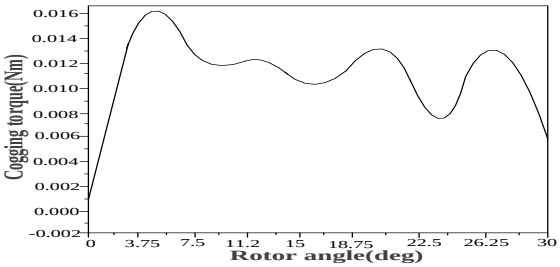

Fig. 16. Combined optimized model for Cogging torque.

The efficiency is 9% for this combined optimized model which is less than that of 2 mm PM height, 5% greater than the 0.82 mm V-shaped rotor pole technique, and 12% less than the 23.5° rotor pole span angle technique [24].

E. Magnet ArrangementMethod

The performance variations in the flux reversal machine (FRM) can be analyzed with various magnet arrangements. Here four PM arrangements are discussed i) NS-SN ii) NS-NS iii) NSNS-SNSN and iv) NSNS-NSNS.

i. NS-SN Magnetic Arrangement

A pair of arc magnets of different polarity is situated beside one other on the surface of every stator-pole. The diametrically opposite stator poles contain the similar polarity in the diametrically opposite permanent magnets. permanent magnets arrangements are shown in fig. 17(a).

ii. NS-NS Magnetic Arrangement

A pair of arc magnets of the same polarity is situated on the surface of everypole of stator. For which the two adjacent magnetic polarities are opposite on different stator teeth. The permanent magnet arrangement shown in fig. 17(b).

iii. NSNS-SNSN magnetic arrangement

Two pairs of arc magnets on one pole of the stator. The two side by side magnets on a different pole of the stator has same polarities. The PM arrangements shown in a fig. 17(c).

iv. NSNS-NSNS magnetic arrangement

The Two pairs of PM magnets are mounted on one pole of the stator. The two side by side magnets on a different pole of the stator has opposite polarities. The PM arrangements shown in a fig. 17(d).

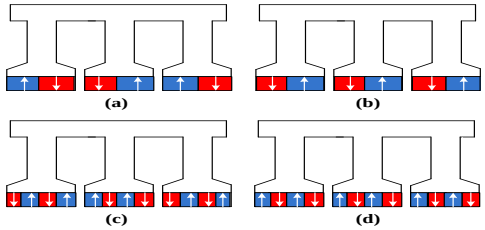

Fig. 17. Various PM Positions.**a)**NS-SN, **b)** NS-NS**, c)** NSNS-SNSN, **d)** NSNS-NSNS.

F. Performance Comparison of PM Arrangements

Comparisons made with different PMs structural arrangements based on performance can be analyzed by slot of the rotor and stator pole combination. The influence of various PMs arrangements on torque and air-gap flux density. By analyzing the torque offering along with the flux density created by the airgap of dominating field harmonics, the effect of PM positions on machine characteristics will be retrieved. Then, consider aexisting 12/14 stator slot and rotor pole machine.

The salient nature of the rotor pole, the MMF is produced by either armature winding or PM in a machine is experienced to changes, leading to huge harmonics. The rotational speed and the number of pole-pairs of the harmonicsdescribed as

$$P_{m,k} = |mp + kN_r| \quad (18)$$

$$\Omega_r = \frac{k\,Nr}{|mp + k\,Nr|} \quad (19)$$

In which p is the number of pole-pairsof armatures-MMF or PM-MMF, m resembles order number, k refers to order of Fourier series of permeance ratio, Nr is the rotor pole number where Ωr is rotational speed of the rotor in mechanical.

The torque is formed by the intervention of dominating filed PMs harmonic pairsand armature fields with the similar rotational speeds and pole-pair numbers. To find the dominating filed working harmonics, the torque influenceof field harmonic is gained using Maxwell tensor, as

$$T_n(t) = \frac{\pi LR^2}{\mu_0} B_{rn} B_{tn} \cos\left[\theta_{rn}(t) - \theta_{tn}(t)\right] \quad (20)$$

Where $T_n(t)$ is the instantaneous torque formed by the n^{th}harmonic, R is the radius of air-gap, L is the axial length, B_{tn} and B_{rn} are the amounts of the tangential and radial apparatuses of the n^{th} harmonic, $\theta_{tn}(t)$ and $\theta_{rn}(t)$are the phases of the tangential and radial components of the n^{th}harmonic, μ_0 is the vacuum permeability.

The torque proportion for four different PMs arrangements of every field harmonic is listed in tables 4 and 5. It gives that the torque of NS-SN is formed by five predominant harmonics for P = $N_s/2$ and only two predominant harmonics results in torque production in NS-NS for P = N_s for 12/14 stator-slots and pole combination.

For NSNS-SNSN, P = $N_s/2$ and averagetorque is obtained by odd-timesharmonics of PM-MMF along with additional harmonics because of rotor tooth changes and torque production for NSNS-NSNS, P = N_s both odd and even harmonics exist. The harmonicsin NSNS-NSNS are extra thanNSNS-SNSN.

Table 4. Percentage of Torque field harmonics in NS-NS and NS-SN (Ns=12, Nr=14).

	P	P-N_r	P+N_r	2P	2P+N_r	3P	3P+N_r
NS NS	12^{th} (88%	2^{nd} (14%	26^{th} (−3%	24^{th} (2%	38^{th} (0%)	36^{th} (−1%)	50^{th} (0%)
NS SN	6^{th} (16%	8^{th} (26%	20^{th} (12%	-	-	18^{th} (−63%	32^{nd} (−2%

Table 5. Torque Percentage of field harmonics in NSNS-SNSN and NSNS-NSNS (Ns=6, Nr=14).

	P	P-N_r	P+N_r	2P	2P+N_r	3P	3P+N_r
NSNS-NSNS	6^{th} (1%)	8^{nd} (1%)	20^{th} (0%)	12^{th} (84%	26^{th} (−2%	18^{th} (9%)	32^{nd} (0%)
NSNS-SNSN	3^{rd} (1%)	11^{th} (2%)	17^{th} (1%)	-	-	9^{th} (13%	23^{rd} (2%)

The torque performance of an FRPMM gets effected prominently by the rotor pole number N_r. Different PM arrangementsexhibits, different torque variation trends, this can be explained by the winding factor of the machine. When N_r varies from 16 to 20, the NS-NS winding factor is more resulting in feasibility to attain high torque and the winding factor of NS-SN is more in the range from 10 to 14, torque the complex torque may produce. However, the torque of NS-SN is less than NS-NS when $N_r = 14$.

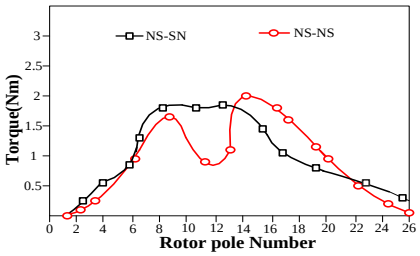

Fig. 18. Changes in Torque across rotor pole number.

For this case NSNS-NSNS and NSNS-SNSN,One another PM arrangements exhibit comparatively more torque while N_r ranges from 10 to 16, and a 14-pole rotor is best for NSNS-NSNS. For NSNS-NSNS, the winding factor is more having $N_r = 14$ and for NSNS-SNSN, when $N_r = 13$ the winding factor is more.

In every machine, the maximum thickness of magnet is estimated approximately as 2 mm [23], so as to improve the anti-demagnetization capacity of the magnets, manufacturing feasibility and to increase the torque. The paths of flux in rotor and stator prominently change with PM arrangement. Various arrangements of PMs have a big impact on the cogging. The cogging torque of NS-NS has the lowest while that of two pairs of magnet pieces arrangements have the largest.

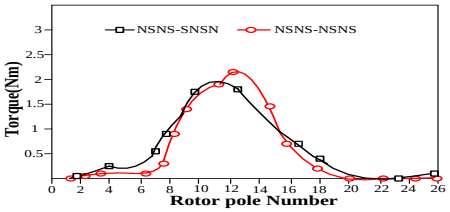

Fig.19. Torque difference against rotor pole number.

The NSNS-NSNS and NSNS-SNSN have higher torque than that of NS-NS and NS-SN irrespective of thevalue of copper loss. Both eddy current and core losses are increased with increased in speed of the magnets rapidly. For the core loss, it is greater in NSNS-NSNS and NSNS-SNSN. For the PM loss, as the magnets are static in nature the eddy currents are produced by all rotatingair-gapharmonics. There are three rotating harmonics in NS-SN with various rotational speeds with the equal frequency and only two spinning harmonics can be in NS-NS. So, the PM loss is lesser in NS-NS than that of NS-SN. The PM loss of NSNS-NSNS is more than that of NSNS-SNSN. In the case of Efficiency, all the machines can exhibit the highest efficiency around 2000 rpm, if the rotor speed getting larger from 2000rpm, the efficiency slowly becomes lesser.

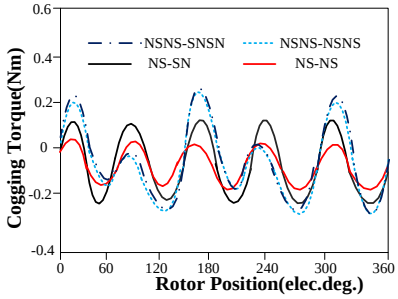

Fig. 20. Cogging torque waveforms of four FRPM machines.

The machine torque of four PM pieces on every stator pole four PM pieces on each stator pole is more than that of machines with two PM pieces. The maximum rotor pole number is approximately 14 for 12 stator slots for FRPMM and these four different PM arrangements are appropriate in a well-defined range of rotor pole number. These optimal alignments can be helpful for design and examining the FRPM machines seeking at a prominent performance.

VI. CONCLUSION

Recent advancements in FRPM machine design flow have been discussed clearly. It is mainly concentrated on performance optimization methods like stator winding and magnetic arrangements are adopted to overcome the disadvantages of a conventional FRPM machine. A qualitative comparison is made between FRPM machine with other brushless machines are analyzed by Flux-MMF diagram technique. The methods explained by the great researchers with experimental results are explained throughout the paper. Although achieving, a basic structure like a traditional FRPM machine is a major task in front of researchers. The work has been carried out by authors towards FRPM machines for renewable harvesting systems.

REFERENCES

1. R. Deodhar, S. Andersson, T. Miller, and I. Boldea, **"**The flux-reversal machine: A new brushless doubly-salient permanent-magnet machine,**"** IEEE Trans. Ind. Appl., vol. 33, no. 4, pp. 925–934, Jul. 1997.
2. Y. Gao, R. Qu, D. Li, J. Li, and L. Wu, "Design of three-phase flux reversal machines with fractional-slot windings," IEEE Trans. Ind. Appl., vol. 52, no. 4, pp. 2856–2864, Jul./Aug. 2016.
3. Boldea, L. Parsa, D. Dorrell, and L. N. Tutelea, "Automotive electric propulsion systems with reduced or no permanent magnets: An overview," IEEE Trans. Ind. Electron., vol. 61, no. 10, pp. 5696–5711, Oct. 2014.
4. D.S. More and B.G. Fernandes, "Analysis of flux-reversal machine based on fictitious electrical gear," IEEE Trans. Energy Convers., vol. 25, no. 4, pp. 940–947, Dec. 2010.
5. Boldea, L. Zhang, and S. A. Nasar, "Theoretical characterization of flux reversal machine in low-speed servo drives-the pole-PM configuration," IEEE Trans. Ind. Appl., vol. 38, no. 6, pp. 1549–1557, Nov./Dec. 2002.
6. D. S. More, H. Kalluru, and B. G. Fernandes, "Comparative analysis of flux reversal machine with fractional slot concentrated winding PMSM," in Proc. IEEE Ind. Electron. Conf., Nov. 2008, pp. 1131–1136.
7. J. Zhang, M. Cheng, Z. Chen, and W. Hua, "Comparison of stator mounted permanent magnet machines based on a general power equation," IEEE Trans. Energy Convers., vol. 24, no. 4, pp. 826–834, Dec. 2009.
8. Z.Q. Zhu and Z. Z. Wu, D.J. Evans, and W.Q. Chu, "Novel electrical machines having separate PM excitation stator," IEEE Trans. Magn., vol.51, no. 4, 2014.
9. Y. S. Kim, T. H. Kim, Y. T. Kim, W. S. Oh, and J. Lee, "Various design techniques to reduce cogging torque in flux-reversal machines," in Proc. 8th Int. Conf. Elect. Mach. Syst., vol. 1, 2005.
10. D. More and B. Fernandes, "Power density improvement of three phase flux-reversal machine with distributed winding," IETJ. Elect. Power-Appl., vol. 4, no. 2, pp. 109–120, Feb. 2010.
11. C. Sikder, I. Husain, and W. Ouyang**,** "Cogging torque reduction in flux-switching permanent-magnet machines by rotor pole shaping," IEEE Trans. Ind. Appl., vol. 51, no. 5, pp. 3609–3619, Sep./Oct. 2015.
12. L. Hao, M. Lin, D. Xu, N. Li, and W. Zhang, "Cogging torque reduction of axial-field flux-switching permanent magnet machine by rotor tooth notching," IEEE Trans. Magn., vol. 51, no. 11, Nov. 2015.
13. T. Kim, S. Won, K. Bong, and J. Lee, "Reduction in cogging torque in flux reversal machine by rotor teeth pairing," IEEE Trans. Magn., vol. 41, no. 10, pp. 3964–3966, Oct. 2005.
14. D. Xu, M. Lin, X. Fu, L. Hao, W. Zhang, and N. Li, "Cogging torque reduction of a hybrid axial field flux-switching permanent magnet machine with three-methods," IEEE Trans. Appl. Super-cond., vol. 26, no. 4, Jun. 2016.
15. D.S. More and B.G. Fernandes, "Analysis of flux-reversal machine based on fictitious electrical gear," IEEE Trans. Energy Convers., vol. 25, no. 4, pp. 940–947, Dec. 2010.
16. R. Qu, D. Li, and J. Wang, "Relationship between magnetic gears and Vernier machines," in Proc. Int. Conf. Elect. Mach. Syst., Beijing, China, 2011.
17. D S Phani Gopal Cheerla, L. Malleswari, and Dr. G. RK Murthy," Mathematical Modelling of Three-Phase Flux Reversal Machine and its simulation." In 1st National Conference on Power Electronics Systems & Applications, PESA 2013.
18. Yuting Gao, Dawei Li, Ronghai Qu, and Jian Li, "Design Procedure of Flux Reversal Permanent Magnet Machines" in IEEE Transactions on industry applications, vol. 53, no. 5, September /October 2017.
19. Boldea, C. Wang, and S. A. Nasar, "Design of a three-phase flux reversal machine," Electrical Machine and Power System, vol. 27, no. 8, pp. 849–863, Aug. 1999.
20. Tae Heoung Kima and Ju Lee," A design technique to improve the performance of flux-reversal machines" in Journal of Applied Physics 97, 2005.
21. Tae Heoung Kim*," A Study on the Iron Loss and Demagnetization Characteristics of an Inset-type Flux-Reversal Machine" in Journal of Magnetics 18(3), 297-301 (2013).
22. Barman D. Sengupta, and Bhattacharya T K**,**" Cogging torque reduction in surface mounted permanent magnet synchronous machine", in IEEE International Conference on Power Electronics, Drives and Energy systems (PEDES) 2016.
23. Li g, Ojeda J, Hlioui S, Hoang E, and Gabsi M, "Modification in rotor pole geometry of mutually coupled switched reluctance machine for torque ripple mitigating". IEEE T magn 2012.
24. Y. Li, Z. Q. Zhu," Influence of Magnet Arrangement on Performance of Flux Reversal Permanent Magnet Machine" Department of Electronic and Electrical Engineering, The University of Sheffield, Sheffield, U.K. IEEE 2017.